Supporting Information

Structural Design for Stretchable Microstrip Antennas

*Jia Zhu, Jake J. Fox, Ning Yi, Huanyu Cheng**

J. Zhu, J. J. Fox, H. Cheng
Department of Engineering Science and Mechanics
The Pennsylvania State University
University Park, Pennsylvania 16802, USA
E-mail: huanyu.cheng@psu.edu

N. Yi, H. Cheng
Department of Materials Science and Engineering
The Pennsylvania State University
University Park, Pennsylvania 16802, USA

H. Cheng
Materials Research Institute
The Pennsylvania State University
University Park, Pennsylvania 16802, USA

Corresponding Author
*E-mail: huanyu.cheng@psu.edu

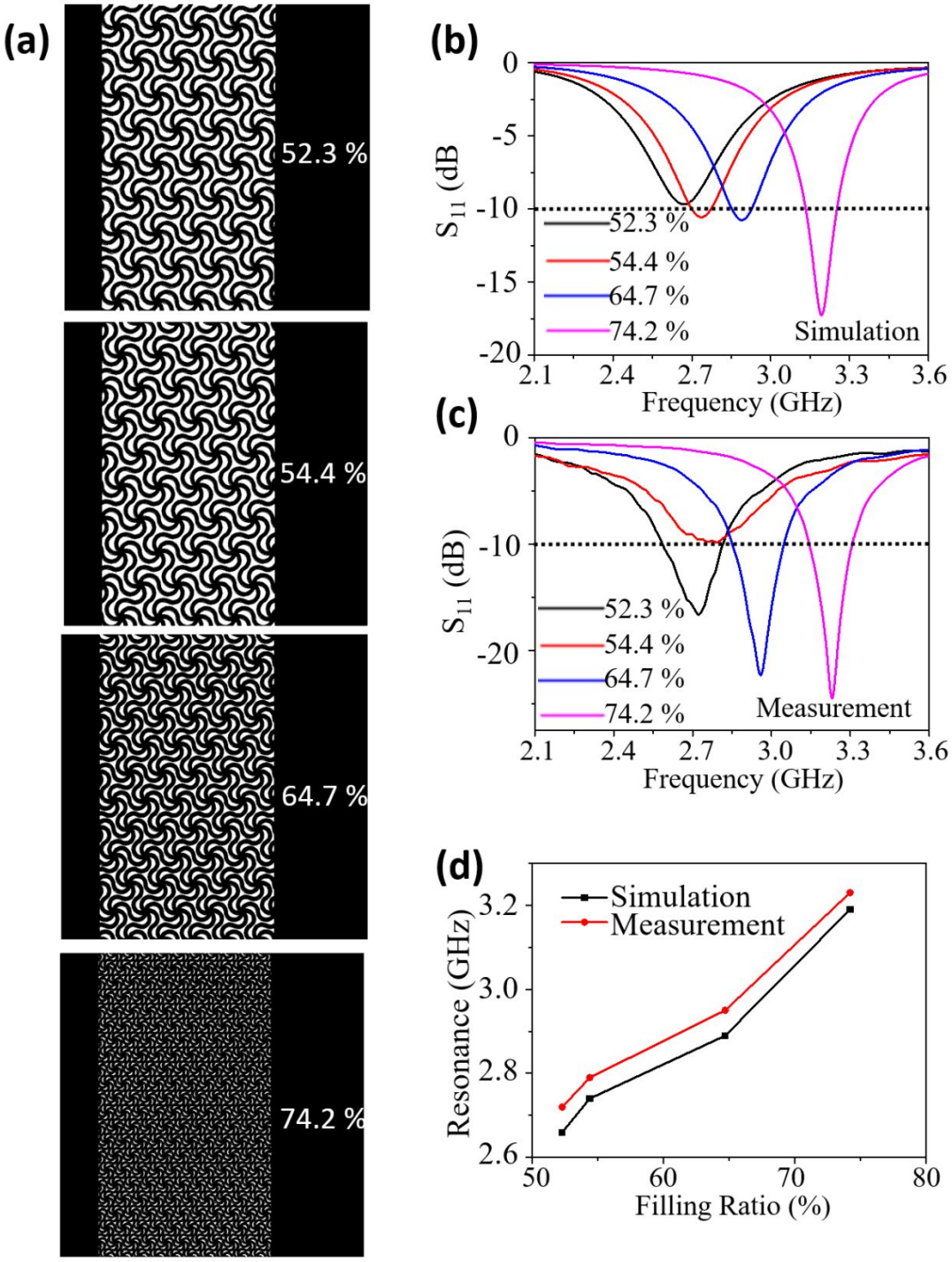

Figure S1 | Effect of the filling ratio in the meshed ground plane. (a) Schematic illustrations of the meshed ground plane with an increasing filling ratio: 52.3 %, 54.4 %, 64.7 %, and 74.2 %. **(b)** Measured and **(c)** simulated S_{11} curves of the antenna that has a solid patch and a meshed ground plane with increasing filling ratio: 52.3 %, 54.4 %, 64.7 %, and 74.2 %. **(d)** The comparison of resonance frequency between the simulation (black) and measurement (red) as a function of filling ratio from 52.3 % to 74.2 %.

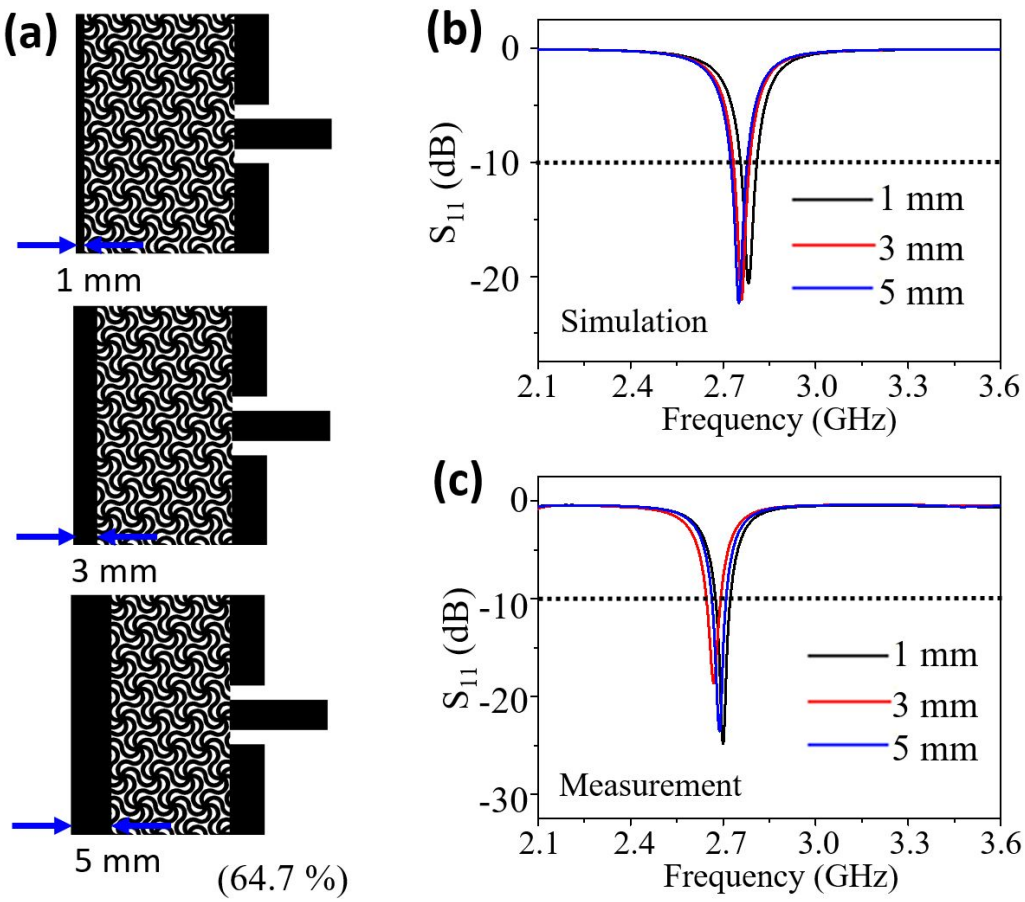

Figure S2 | Effect of the solid edge width. (a) Schematic illustrations of the meshed ground plane with a filling ratio of 64.7 %, but an increasing edge width: 1 mm, 3 mm, and 5 mm. **(b)** Measured and **(c)** simulated S_{11} curves of the antenna that has a solid patch and a meshed ground plane with an increasing edge width: 1 mm, 3 mm, and 5 mm.

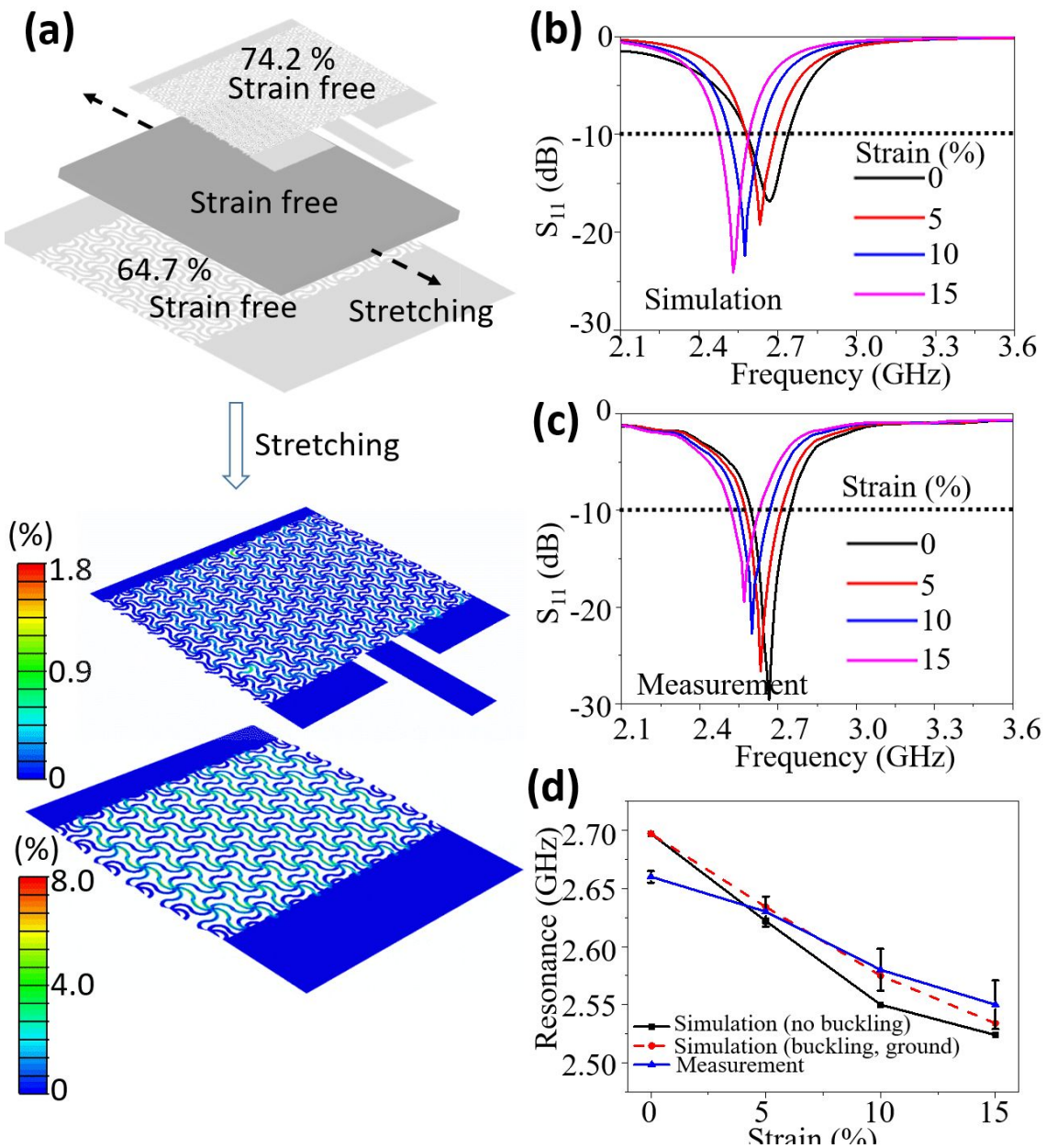

Figure S3 | Design and performance of the meshed microstrip antenna with different filling ratios in the meshed patch and meshed ground plane. (a) Strain distribution in the meshed microstrip antenna with a meshed patch (filling ration of 74.2 %) and a meshed ground plane (filling ration of 64.7 %) before and after a tensile strain of 15 %. **(b)** Simulated and **(c)** measured S_{11} curve of the meshed microstrip antenna. The thickness of the dielectric substrate was measured to be 1.5 mm, which was used in the simulation that also considered the out-of-plane buckling of the serpentine network in the meshed ground plane. **(d)** The comparison of resonance frequency between the simulation (solid lines) and measurement (dashed line) for a tensile strain from 0 % to 15 %. The simulation result that does not consider buckling was also plotted for comparison. The buckling in the meshed ground plane was also shown to be small.

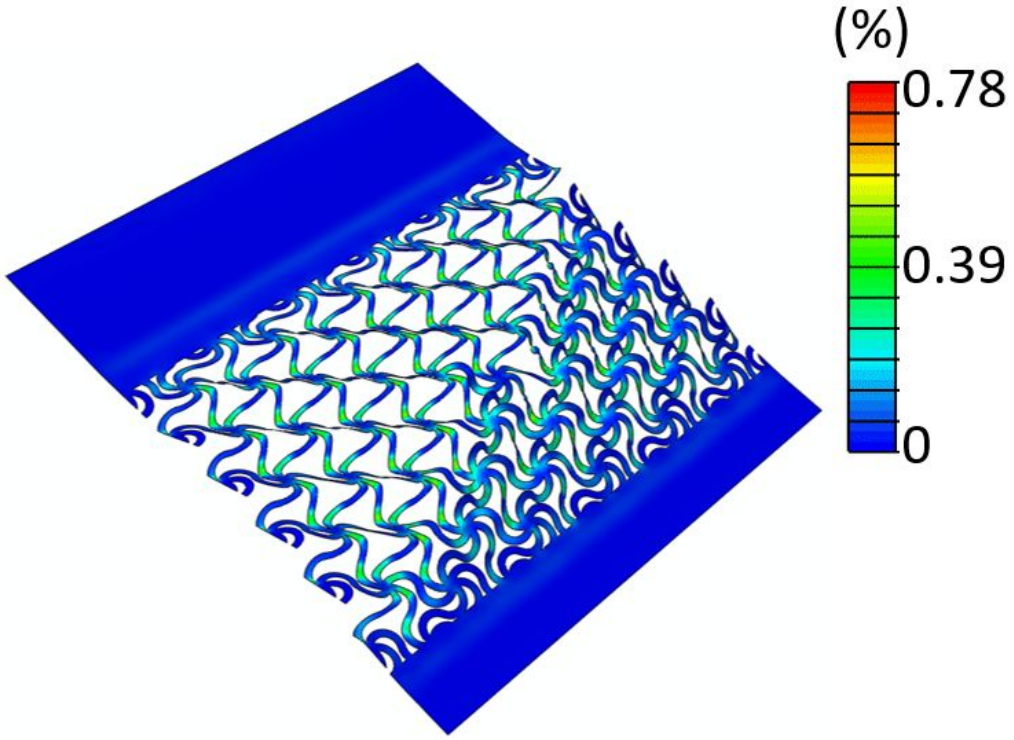

Figure S4 | Strain distribution of a meshed ground plane with a filling ratio of 64.7 % under a tensile strain of 15 % stretching when the out-of-plane buckling was considered.

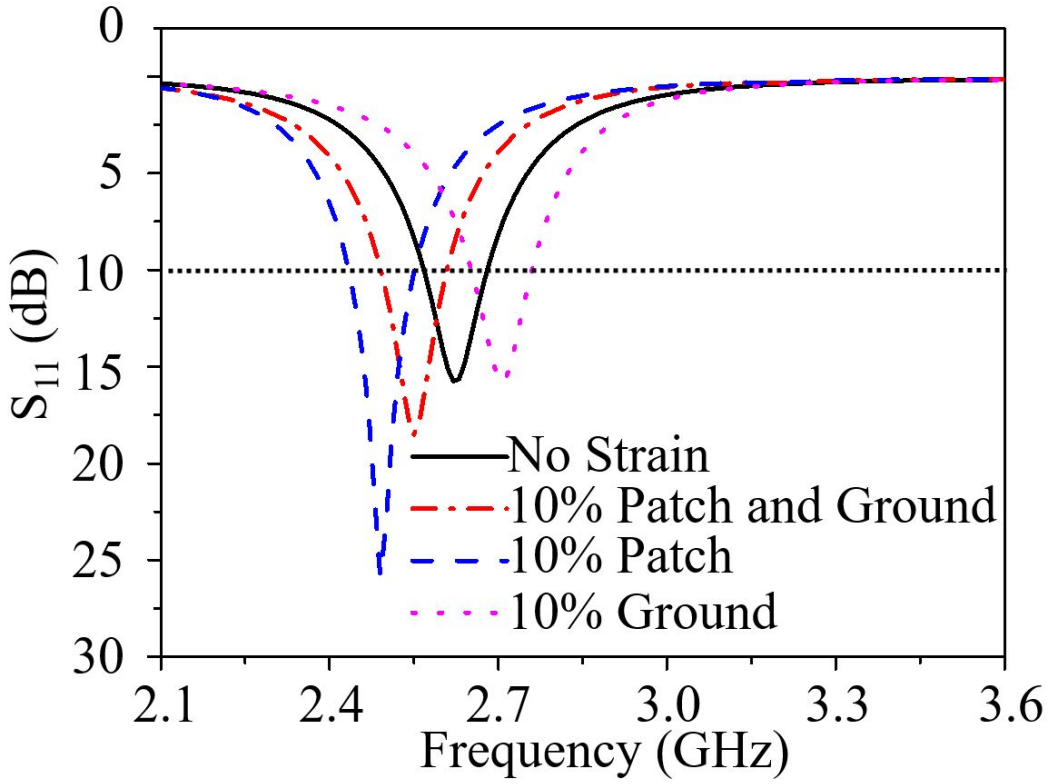

Figure S5 | Simulated S_{11} curves of the meshed microstrip antennas with a meshed patch (filling ratio of 74.2 %) and a ground plane (filling ratio of 64.7 %) that are separately stretched to demonstrate the influence of each on the resonance frequency. Black solid line: 0 % strain on both the meshed patch and meshed ground plane. Blue dashed line: a tensile strain of 10 % on the meshed patch and 0% on the meshed ground plane. Magenta dashed line: a tensile strain of 10 % on the meshed patches and 10% on the ground plane. Red dashed line: a tensile strain of 10 % on both the meshed patch and the meshed ground plane.

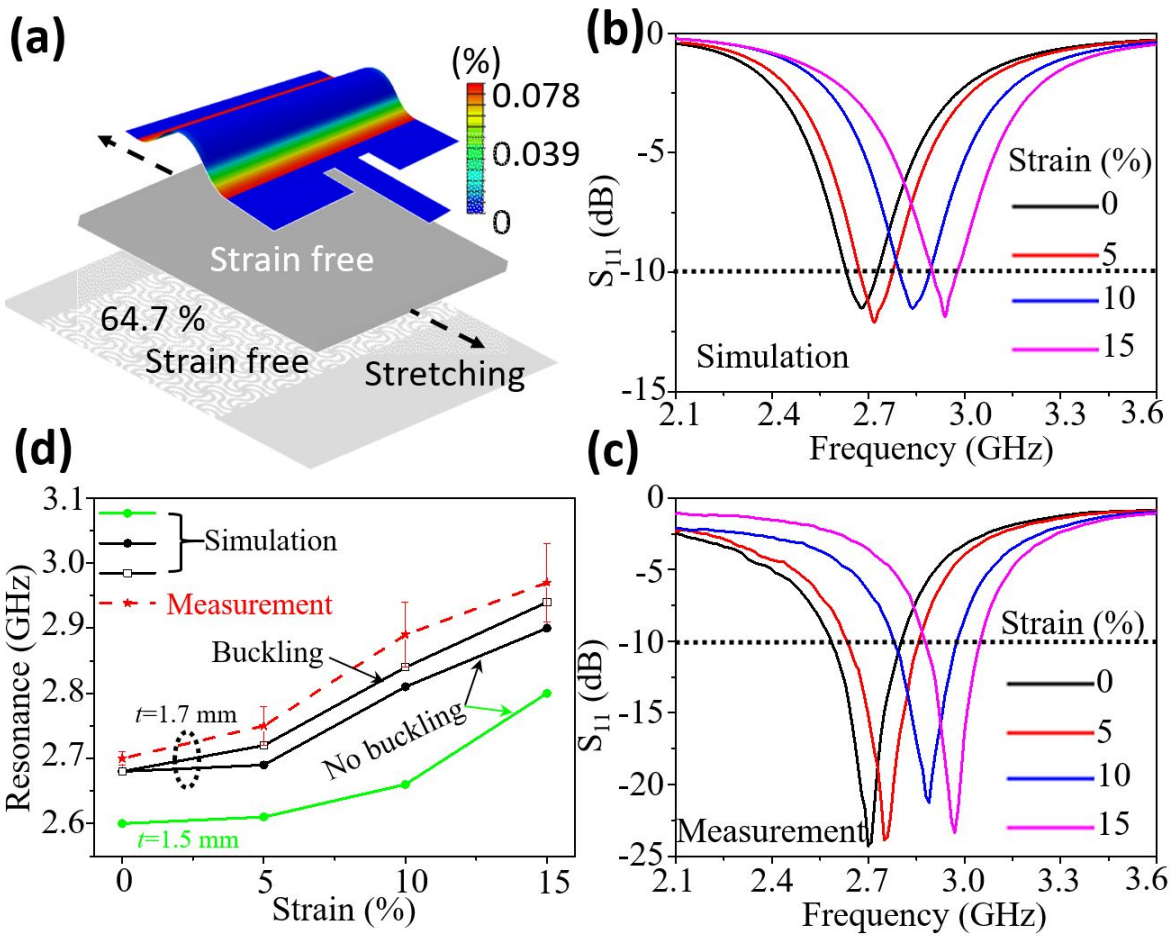

Figure S6 | Design and performance of the arched microstrip antenna that has a meshed ground plane with a filling ratio of 64.7 %. (a) Strain distribution in the resulting arched microstrip antenna before and after a tensile strain of 15 %. **(b)** Simulated and **(c)** measured S_{11} curve of the arched microstrip antenna. The thickness of the dielectric substrate was measured to be 1.7 mm, which was used in the simulation that also considered the out-of-plane buckling of the serpentine network in the meshed ground plane. **(d)** The comparison of resonance frequency between the simulation (solid lines) and measurement (dashed line) for a tensile strain from 0 % to 15 %. The simulation results that do not consider buckling (with a dielectric substrate of 1.7 mm and 1.5 mm) were also plotted for comparison. The thickness of the dielectric substrate was shown to have a large effect on the resonance frequency, where the role of the buckling in the meshed ground plane was relatively small.

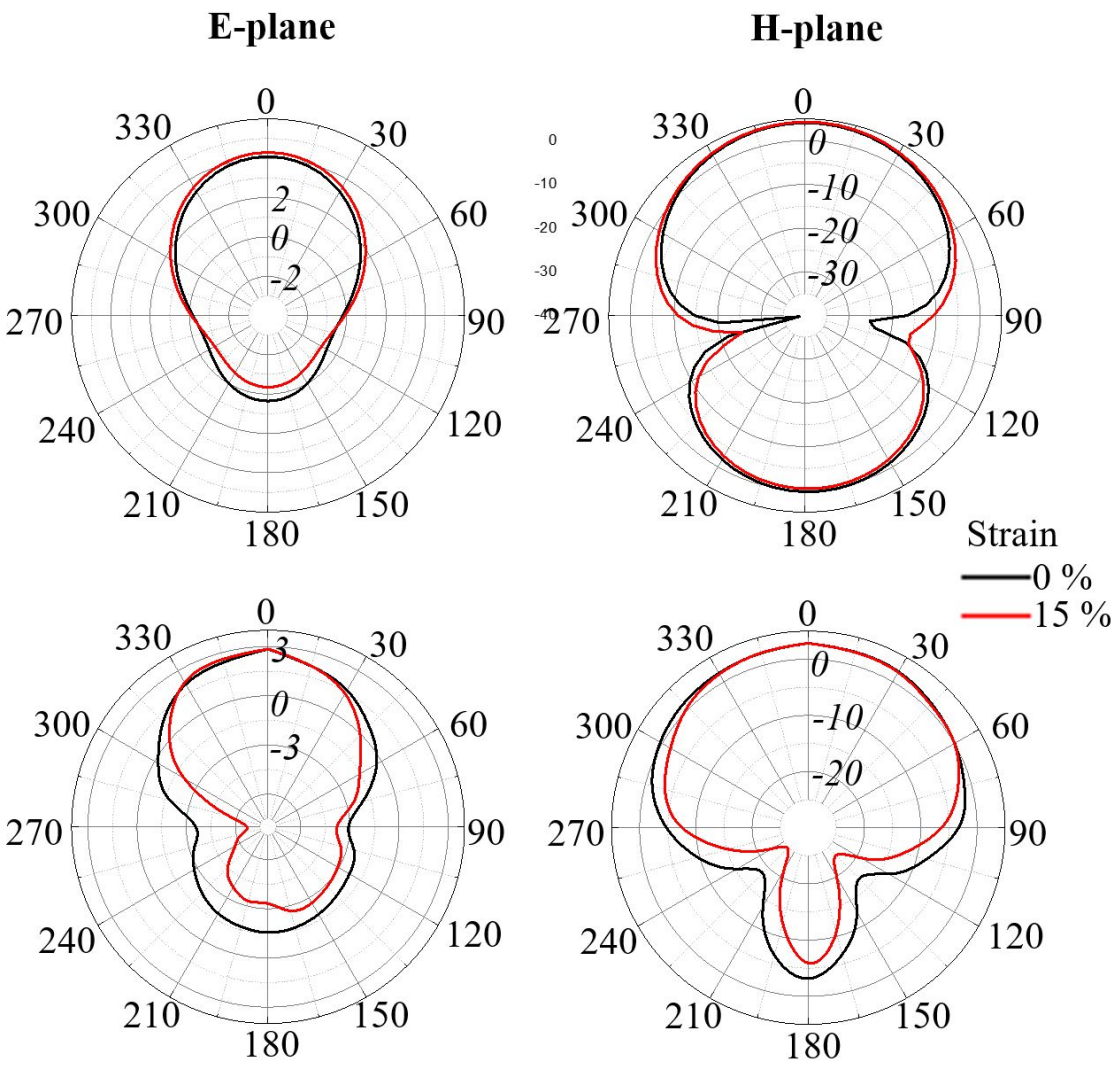

Figure S7 | The comparison of the normalized radiation patterns in the (right) E-plane and (left) H-plane between the (top) simulated and (bottom) measured results for the stretchable arched microstrip antenna with a filling ratio of 64.7 % for the meshed ground plane. The externally applied tensile strain of 0 % and 15 % were denoted in black and red, stretching.

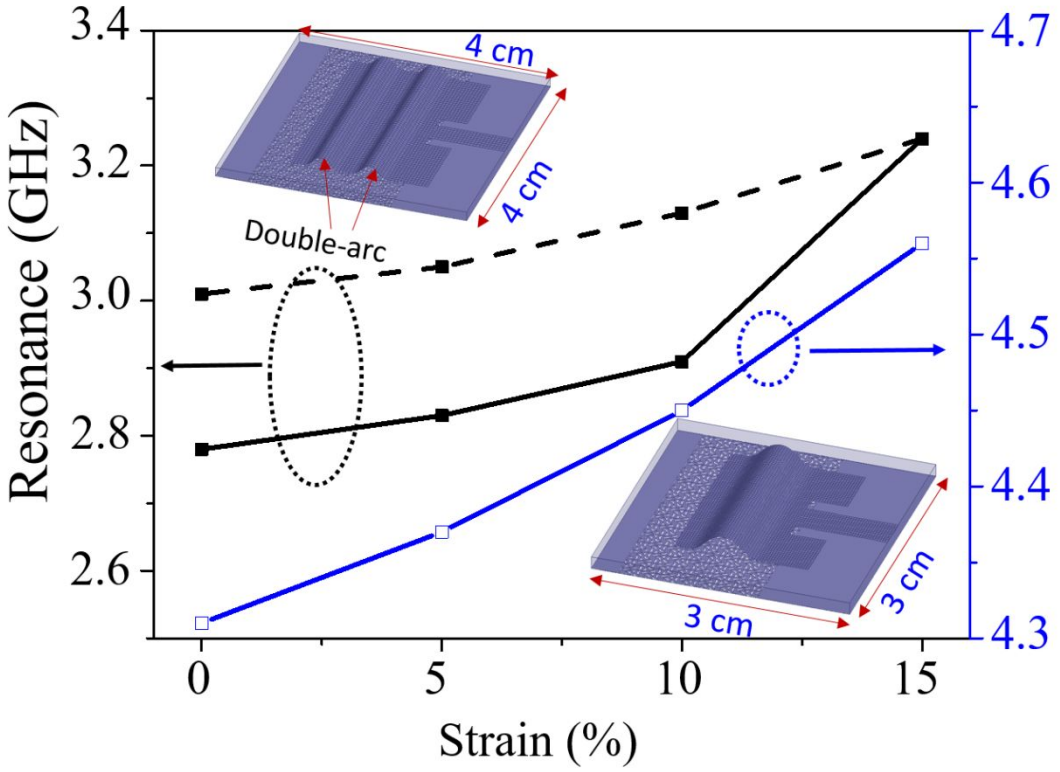

Figure S8 | Change of resonance frequency in the stretchable arched antenna with (left axis, black) a different number of arcs (one vs. two arcs) and (right axis, blue) different lateral dimensions (3 cm by 3 cm as opposed to 4 cm by 4 cm shown on the left axis).

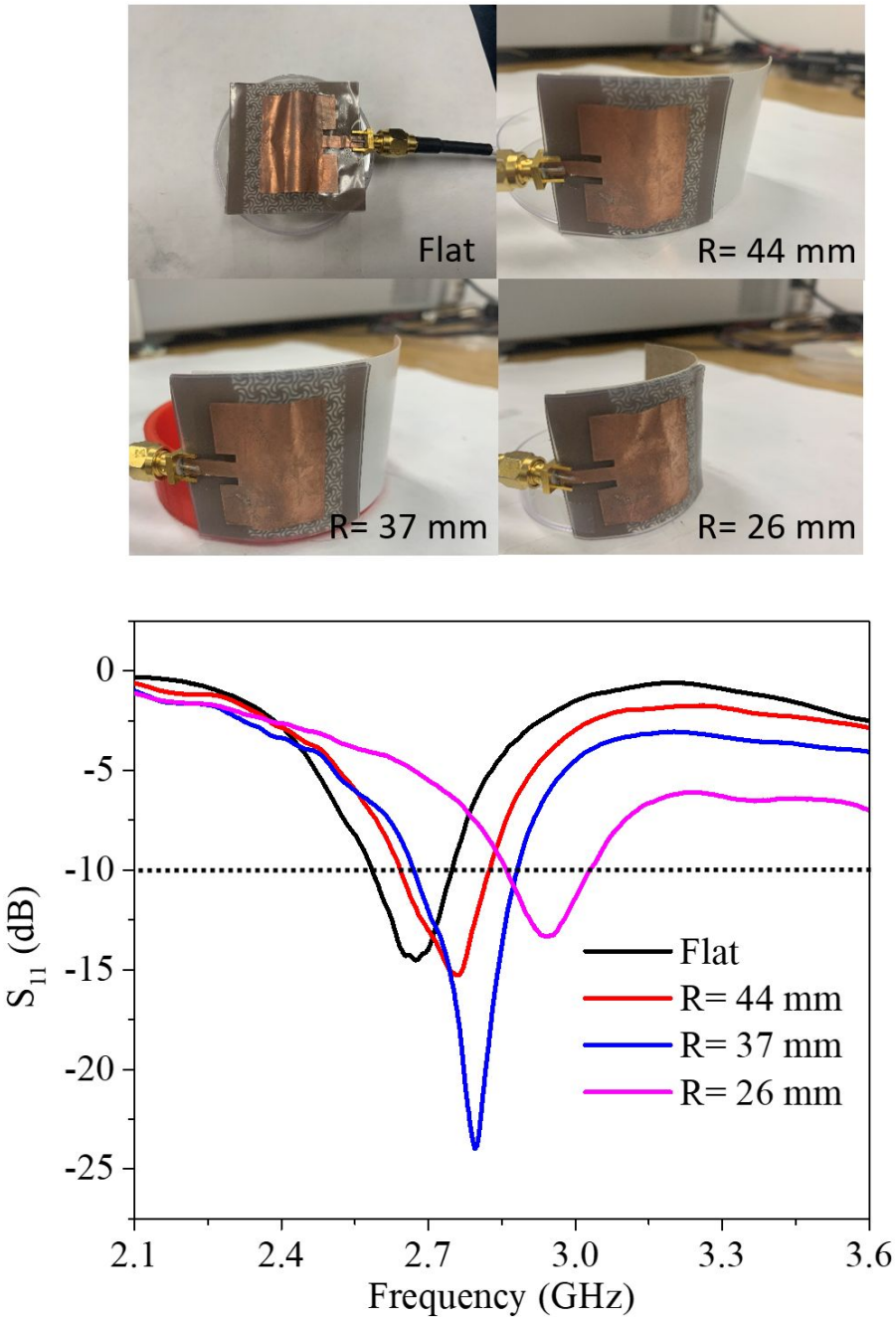

Figure S9 | Bending demonstration of the arched microstrip antenna. (a) Optical images of the arched microstrip antenna bent over cylinders with various radii of curvature. **(b)** Measured S_{11} curves as a function of the radius of curvature.

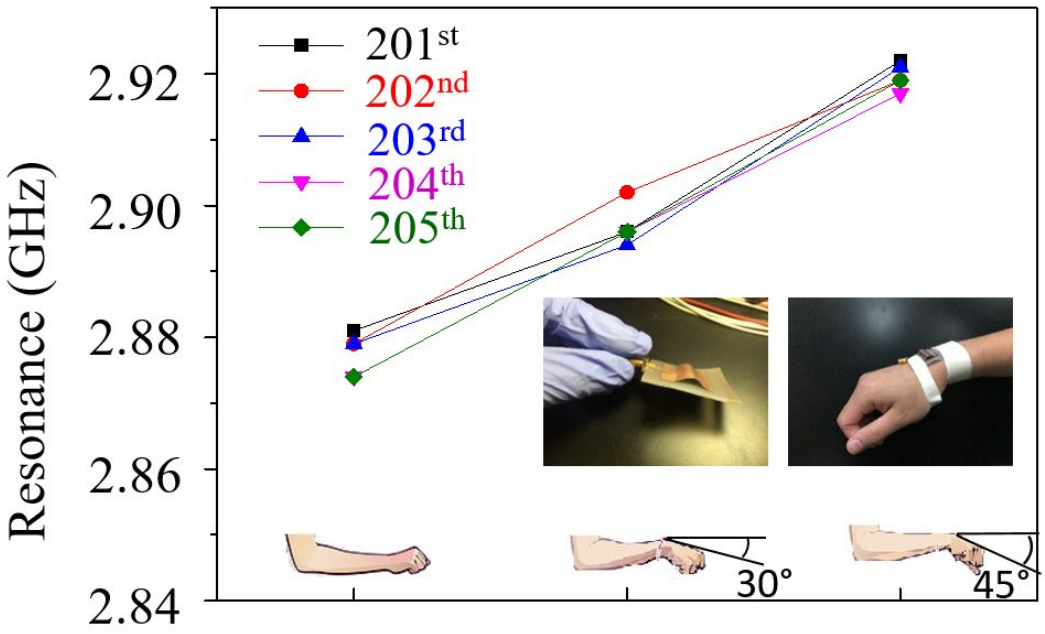

Figure S10 | Cycling performance of the motion detection sensor was demonstrated by measuring the change in the resonance frequency for 5 consecutive cycles of bending and recovering after 200 cycles.